Published in final edited form as:

J Steroid Biochem Mol Biol. 2018 March ; 177: 59–69. doi:10.1016/j.jsbmb.2017.07.011.

Properties of Purified CYP2R1 in a Reconstituted Membrane Environment and its 25-Hydroxylation of 20-Hydroxyvitamin D3

Chloe Y. S. Cheng[a], **Tae-Kang Kim**[b], **Saowanee Jeayeng**[b,d], **Andrzej T. Slominski**[b,c], and **Robert C. Tuckey**[a]

[a]School of Molecular Sciences, The University of Western Australia, Perth, WA 6009, Australia [b]Department of Dermatology, University of Alabama at Birmingham, AL 35294, USA [c]VA Medical Center, Birmingham, AL 35294, USA [d]Department of Pharmacology, Faculty of Medicine Siriraj Hospital, Mahidol University, Bangkok 10700, Thailand

Abstract

Recent studies indicate that CYP2R1 is the major 25-hydroxylase catalyzing the first step in vitamin D activation. Since the catalytic properties of CYP2R1 have been poorly studied to date and it is a membrane protein, we examined the purified enzyme in a membrane environment. CYP2R1 was expressed in *E. coli* and purified by nickel affinity- and hydrophobic interaction-chromatography and assayed in a reconstituted membrane system comprising phospholipid vesicles plus purified human NADPH-P450 oxidoreductase. CYP2R1 converted vitamin D3 in the vesicle membrane to 25-hydroxyvitamin D3 [25(OH)D3] with good adherence to Michaelis-Menten kinetics. The kinetic parameters for 25-hydroxylation of vitamin D3 by the two major vitamin D 25-hydroxylases, CYP2R1 and CYP27A1, were examined in vesicles under identical conditions. CYP2R1 displayed a slightly lower k_{cat} than CYP27A1 but a much lower K_m for vitamin D3, and thus an overall 17-fold higher catalytic efficiency (k_{cat}/K_m), consistent with CYP2R1 being the major vitamin D 25-hydroxylase. 20-Hydroxyvitamin D3 [20(OH)D3], the main product of vitamin D3 activation by an alternative pathway catalyzed by CYP11A1, was metabolized by CYP2R1 to 20,25-dihydroxyvitamin D3 [20,25$(OH)_2$D3], with catalytic efficiency similar to that for the 25-hydroxylation of vitamin D3. 20,25$(OH)_2$D3 retained full, or somewhat enhanced activity compared to the parent 20(OH)D3 for the inhibition of the proliferation of melanocytes and dermal fibroblasts, with a potency comparable to 1,25-dihydroxyvitamin D3 [1,25$(OH)_2$D3]. The 20,25$(OH)_2$D3 was also able to act as an inverse agonist on retinoic acid-related orphan receptor α, like its parent 20(OH)D3. Thus, the major findings of this study are that CYP2R1 can metabolize substrates in a membrane environment, the enzyme displays higher catalytic efficiency than CYP27A1 for the 25-hydroxylation of vitamin D, it efficiently

Address for correspondence: Robert C. Tuckey, PhD, School of Molecular Sciences, The University of Western Australia, Perth, WA, 6009, Australia, Tel: 61 8 64883040, Fax: 61 8 30401148, robert.tuckey@uwa.edu.au.

Conflict of Interest:
The authors declare no conflict of interest

hydroxylates 20(OH)D3 at C25 and this product retains the biological activity of the parent compound.

Keywords

CYP2R1; Vitamin D3; 25-hydroxylase; Phospholipid vesicles

1. Introduction

Vitamin D is an inactive prohormone formed in the skin by UV-irradiation of 7-dehydrocholesterol, followed by thermal isomerization of the resulting pre-vitamin D (1–3). 1α,25-dihydroxyvitamin D [1,25$(OH)_2$D] is the major physiologically active form of vitamin D and is responsible for maintaining calcium homeostasis (3). 1,25$(OH)_2$D also displays other properties such as inhibition of cell proliferation of normal and cancer cells, promotion of differentiation, modulation of the immune system, and reduction of fibrosis (3–6). Its effects are mediated by binding to the vitamin D receptor (VDR) (7–10). The activation of vitamin D to 1,25$(OH)_2$D is a two-step process which first involves 25-hydroxylation in the liver, followed by 1α-hydroxylation by CYP27B1 in the kidneys (1,11,12). Early studies showed that both microsomal and mitochondrial fractions of the liver exhibit vitamin D3 25-hydroxylase activity, mediated by P450 enzymes (13–16). CYP27A1 was identified originally as the mitochondrial P450 responsible for 25-hydroxylation of vitamin D3 (14,17,18). Cheng *et al.* (19) later identified the microsomal P450, CYP2R1, as a microsomal P450 that could hydroxylate vitamin D3 at C25. Genetic studies have shown that despite a reduction in bile acid synthesis, 25-hydroxyvitamin D [25(OH)D] levels were maintained in CYP27A1-deficient individuals and mice. In contrast, mutations in the CYP2R1 gene result in individuals having insufficient levels of 25(OH)D or lower than normal serum calcium levels, indicating its physiological importance (17,19–21).

An alternative pathway of vitamin D3 activation is catalyzed by CYP11A1, a mitochondrial cytochrome P450 best known for its involvement in steroid synthesis, and produces 20-hydroxyvitamin D3 [20(OH)D3] as the major product (22–26). 20(OH)D3 acts as a biased agonist on the VDR, and as an inverse agonist on the retinoic acid-related orphan receptors α and γ (RORα,γ), members of the nuclear receptor family (27–29). Through modulation of these receptors, 20(OH)D3 displays many properties similar to 1,25$(OH)_2$D3, but without causing hypercalcemia at high doses or causing marked induction of CYP24A1 expression (29–34). Unlike vitamin D3, 20(OH)D3 serves as a substrate for CYP3A4, a major liver microsomal P450, which converts it to 20,24*R*-dihydroxyvitamin D3 [20,24*R*$(OH)_2$D3], 20,24*S*-dihydroxyvitamin D3 [20,24*S*$(OH)_2$D3] and 20,25-dihydroxyvitamin D3 [20,25$(OH)_2$D3] (35,36). These dihydroxyvitamin D3 metabolites have also been shown to be biologically active, reducing colony formation by melanoma cells, inhibiting keratinocyte proliferation and inhibiting IFNγ production to reduce inflammation (28,36–38). 20(OH)D3 and some of its metabolites have been detected in human serum, indicating a possible physiological role (39).

Studies on the catalytic properties of CYP2R1 are limited to date. CYP2R1 has been expressed in a yeast system, where the microsomal fraction was isolated and assayed. This revealed that CYP2R1 can hydroxylate both vitamin D3 and D2 at C25, with the catalytic efficiency for vitamin D3 being about double that for vitamin D2 (40). In more recent work, CYP2R1 has been expressed in *E. coli*, extracted and purified by nickel-affinity and ion-exchange chromatography. Activity measurements showed that the expressed enzyme could metabolize vitamin D3, 1-hydroxyvitamin D3 and 1-hydroxyvitamin D2 at similar rates to those reported for the yeast system (41). The crystal structure of the expressed CYP2R1 in complex with vitamin D3 was determined which indicated that the vitamin D access channel faces the hydrophobic domain of the membrane (41), consistent with other microsomal P450s (42). The aim of our study was to characterize the properties of bacterially expressed and purified CYP2R1 in a reconstituted membrane environment resembling its native environment in the microsomal membrane, and secondly, to determine its ability to metabolize 20(OH)D3 to 20,25$(OH)_2$D3, and test the biological activity of this product.

2. Materials and methods

2.1. Materials

Adenosine 2′,5′-diphosphate agarose, octyl-sepharose CL-4B, glucose-6-phosphate, glucose-6-phosphate dehydrogenase, vitamin D3, dioleoyl phosphatidylethanolamine (DOPE), dimyristoyl phosphatidylcholine (DMPC) and cytochrome b_5 were purchased from Sigma Aldrich (NSW, Australia). DE52 cellulose was purchased from Whatman Inc (NJ, USA) and Ni-NTA His-band resin was from Merck Millipore (VIC, Australia). Dioleoyl phosphatidylcholine (DOPC) and bovine heart cardiolipin were from Avanti Polar Lipids, Inc. (Alabama, USA), and 2-hydroxypropyl-β-cyclodextrin (HP-β-CD) was from Cerestar (Hammond, IN). Prestained broad-range molecular weight markers and mini-PROTEAN TGX precast 12% polyacrylamide gels were from Bio-Rad Laboratories Pty., Ltd. (NSW, Australia). All solvents used were of HPLC grade and purchased from Merck (Darmstadt, Germany). The LanthaScreen TR-FRET RORα Coactivator kit was from Thermo Fisher Scientific, Inc., Waltham, MA. Human CYP2R1 cDNA containing a replaced N-terminal transmembrane anchor domain (with MAKKT), subcloned into the pCW-LIC vector has been described before (41) and was provided by Dr Natallia Strushkevich (Institute of Bioorganic Chemistry, National Academy of Sciences of Belarus). The pGro7 plasmid encoding chaperonins GroEL/ES which assist protein folding, was from Takara Bio Inc. (Otsu, Japan). The plasmid encoding human NADPH-P450 oxidoreductase (POR) has been described before (43) and was provided by Dr Elizabeth Gillam (University of Queensland, Australia). CYP27A1 used in this study was expressed in *E. coli* JM109 cells and purified as described previously (44).

2.2. Expression and purification of hCYP2R1

Competent *E. coli* JM109 cells were transformed with the human CYP2R1 plasmid and pGro7 (encoding GroEL/ES) as described previously (45), and cultures were grown at 37°C to an absorbance of 1.0 at 600 nm. L-Arabinose (4 mg/mL), isopropyl-β-D-thiogalactopyranoside (1 mM) and δ-aminolevulinic acid (0.5 mM) were added to the cultures which were further incubated at 26°C for 42 h with shaking (220 rpm) (46). The *E.*

coli cells were harvested by centrifugation (2,500 × *g*) for 20 min at 4°C and resuspended in buffer comprising 100 mM potassium phosphate, 0.1 mM EDTA, 0.1 mM DTT, 0.1 mM phenylmethanesulfonyl fluoride (PMSF) and 20% (v/v) glycerol. CYP2R1 was extracted from the resuspended cells with 1% (w/v) CHAPS and lysozyme (100 μg/mL), similar to that described for CYP27B1 (46), and then sonicated on ice five times for 40 s each at 40% amplitude using a Vibra-Cell Ultrasonic Processor with a 1.2 cm probe (Sonics and Materials, Inc., Newtown, CT), with 2 min cooling intervals. Cell debris was then removed by centrifugation (104,600 × *g*) for 1 h at 4°C.

Membrane and cytosol fractions of *E. coli* were prepared in order to ascertain the distribution of CYP2R1 between these fractions. *E. coli* cells transformed with the CYP2R1 plasmid were grown as described above and harvested by centrifugation (2,500 × *g*) for 20 min at 4°C. The resulting cell pellet was then resuspended in buffer comprising 10 mM Tris-HCl and 0.75 M sucrose, and incubated with lysozyme (100 μg/mL) for 30 min, followed by centrifugation (4,720 × *g*) for 20 min at 4°C. The pellet was resuspended in buffer comprising 20 mM potassium phosphate, 0.1 mM EDTA, 0.1 mM DTT and 0.1 mM PMSF, and sonicated on ice six times for 40 s at 40% amplitude, with 2 min cooling intervals, then centrifuged (104,600 × *g*) for 1 h at 4°C to sediment the membrane fraction. CO-reduced minus reduced difference spectroscopy was carried out on the supernatant and resuspended pellet (membrane fraction) to determine P450 content present in each.

CYP2R1 was initially purified from the CHAPS extract of resuspended *E. coli* cells from 1.5 L of culture using nickel-affinity chromatography, as described for CYP27B1 (46), on a column (1.5 × 5.0 cm, Ni-NTA His-band resin) equilibrated with buffer A (50 mM sodium phosphate, 0.3 M NaCl, 0.1 mM PMSF, 20% (v/v) glycerol and 0.05% CHAPS). The column was then washed with 100 mL buffer A followed by 300 mL buffer A containing 50 mM imidazole. CYP2R1 was eluted with 200 mM imidazole in buffer A, and then dialyzed overnight at 4°C against 25 volumes buffer B (50 mM sodium phosphate, 0.3 M NaCl, 0.1 mM PMSF, 20% (v/v) glycerol and 0.01% CHAPS) to reduce imidazole and CHAPS concentrations. Nickel-affinity chromatography was repeated on the dialyzed fraction. The CYP2R1 was then applied to an octyl-Sepharose column (1 × 5 cm), equilibrated with buffer C (20 mM potassium phosphate, 0.1 mM EDTA, 0.1 mM DTT, 20% (v/v) glycerol) plus 0.05% CHAPS. The column was washed with three column volumes of buffer C, followed by 50 mL 0.1% CHAPS then 100 mL 0.2% CHAPS in buffer C. CYP2R1 was eluted with 1% CHAPS in buffer C and dialyzed overnight at 4°C against 20 volumes buffer C plus 0.3 M NaCl. The P450 concentration was estimated from a CO-reduced minus reduced difference spectrum at 446 and 490 nm with the extinction coefficient of 91,000 $M^{-1}cm^{-1}$.

2.3. Expression and purification of human POR

E. coli JM109 cells were transformed with the human POR plasmid as described previously (43) and pGro7, and cultures were grown at 37°C to an absorbance of 1.0 at 600 nm. L-Arabinose (4 mg/mL) and isopropyl-β-D-thiogalactopyranoside (1 mM) were added and cultures incubated at 26°C for 42 h with shaking at 220 rpm. The cells were harvested by centrifugation (2,500 × *g*) for 20 min and the membrane fraction prepared in buffer comprising 10 mM Tris-HCl and 0.75 M sucrose, and incubated with lysozyme (100 μg/mL)

for 30 min before centrifugation (4,720 × *g*) for 20 min. The pellet was resuspended in buffer comprising 20 mM potassium phosphate, 0.1 mM EDTA, 0.1 mM DTT, 0.1 mM PMSF then sonicated on ice six times using a Vibra-Cell Ultrasonic Processor (described above) for 40 s each at 40% amplitude, with 2 min cooling intervals, then centrifuged (104,600 × *g*) for 1 h to collect the membranes. POR was solubilized from the resuspended membranes with 1% Triton X-100 for 1 h and membrane remnants removed by centrifugation (104,600 × *g*) for 1 h.

Purification of POR was based on that described previously for rat NADPH-cytochrome P450 reductase (47). The extracted POR was initially purified by NADP-affinity chromatography, on a column (1 × 4 cm, adenosine 2′,5′-diphosphate agarose gel) equilibrated with buffer D (75 mM potassium phosphate and 0.025% Triton X-100). The Triton X-100 extract was applied to the column which was then washed with 100 mL buffer D, and eluted with 200 mg/L $NADP^+$ in buffer D. Fractions containing POR from spectral scans (300 – 700 nm) were pooled and the POR further purified by anion-exchange chromatography, using a diethylaminoethyl (DE-52) cellulose column (1 × 5 cm,) equilibrated with buffer C plus 0.025% Triton X-100. The column was then washed with buffer C plus 0.025% Triton X-100 followed by 100 mL 0.05 M NaCl, 50 mL 0.1 M NaCl in buffer C plus 0.025% Triton X-100. The POR was eluted with 0.3 M NaCl in buffer C plus 0.025% Triton X-100. The concentration of purified POR was estimated using a molar extinction coefficient of 21,400 $M^{-1}cm^{-1}$ at 456 nm, as described previously (47).

2.4. SDS-PAGE analysis

The purity of CYP2R1 and POR was analyzed by electrophoresis on a 12% polyacrylamide precast gel (Bio-Rad). The Ponceau S protein assay (48) was used to estimate the amount of total protein in fractions. Protein samples (0.25 or 5 μg) were prepared in SDS-sample buffer and loaded onto the gel and electrophoresis was carried out in SDS-running buffer at 150 V and the gel stained with Coomassie blue, as described previously (49).

2.5. Metabolism of vitamin D3 and 20(OH)D3 by CYP2R1 in phospholipid vesicles

Vitamin D3 or 20(OH)D3 was incorporated into phospholipid vesicles comprising DOPC (1.08 μmol) and bovine heart cardiolipin (0.19 μmol) at a concentration of 0.1 mol per mol of phospholipid (PL), unless otherwise specified. The vesicles were prepared by first removing ethanol solvent under nitrogen then adding 0.5 mL buffer comprising 20 mM HEPES pH 7.4, 100 mM NaCl, 0.1 mM EDTA and 0.1 mM DTT to the substrate and phospholipid mixture which was then sonicated for 10 min in a bath-type sonicator (50). Vesicles (510 μM phospholipid) were incubated with CYP2R1 (0.25 μM) in the same buffer used for vesicle preparation, along with 500 μM NADPH, 2 mM glucose-6-phosphate, 2 U/mL glucose-6-phosphate dehydrogenase and 1.0 μM POR. To compare the effects of phospholipid composition, vesicles comprising DOPE (0.36 μmol) and DOPC (0.91 μmol), DOPC only (1.27 μmol), or DMPC only (1.27 μmol) were prepared with vitamin D3 as described above. In the comparison of assay systems, vitamin D3 (50 μM) was added to the reaction mixture from 4.5% HP-β-CD or ethanol stocks, as described before (36,41,51). Tubes containing the reaction mixture (0.5 mL) were pre-incubated for 8 min in a 37°C shaking water bath, then reactions started by the addition of POR. Where present,

cytochrome b_5 (see Results for concentrations) was included in the pre-incubation and the reaction was started by the combined addition of NADPH and POR. Reactions were carried out at 37°C with shaking (see Results for times) before being terminated by the addition of 2.5 vol ice-cold dichloromethane. Tubes were centrifuged (670 × *g*) for 10 min and the lower organic phase was removed and retained, while the upper aqueous phase was extracted twice more with 2.5 vol dichloromethane. The extracted secosteroids were dried under nitrogen gas at 30°C and dissolved in the solvent required for HPLC analysis (see section 2.7) and stored at −20°C.

2.6. Metabolism of vitamin D3 by CYP27A1 in phospholipid vesicles

Vitamin D3 was incorporated into phospholipid vesicles comprising DOPC and cardiolipin as described in section 2.5. Vesicles (510 μM phospholipid) were incubated with CYP27A1 (0.2 μM) in the same buffer used for vesicle preparation, along with 2 mM glucose-6-phosphate, 2 U/mL glucose-6-phosphate dehydrogenase, 50 μM NADPH, 15 μM human adrenodoxin and 0.4 μM human adrenodoxin reductase, as before (44). Tubes containing the reaction mixture were pre-incubated for 6 min in a 37°C shaking water bath and the reactions started by the addition of adrenodoxin. Reactions were carried out for 10 min at 37°C before being terminated by the addition of 2.5 vol ice-cold dichloromethane. Secosteroids were extracted and prepared for HPLC analysis as described above (Section 2.5).

2.7. Analysis of metabolites by reverse-phase HPLC

The metabolites produced from CYP2R1 or CYP27A1 action on vitamin D3 or 20(OH)D3 were analysed using a Perkin Elmer HPLC system (Flexar Binary Pump Series 200) with a UV detector set at 265 nm, equipped with a C18 column (Grace Alltima, 25 cm × 4.5 mm, particle size 5 μm). The HPLC method used consisted of an initial 64 – 100% methanol in water gradient for 15 min, followed by 100% methanol for 40 min, at a flow rate of 0.5 mL/min. To confirm product identity in a different solvent system, an acetonitrile gradient was used consisting of an initial 45 – 100% acetonitrile in water gradient for 30 min, followed by 100% acetonitrile for 35 min, at flow rate of 0.5 mL/min. Metabolite peaks were integrated and calculated as a percentage conversion of substrate, and where appropriate, kinetic parameters determined by fitting the Michaelis-Menten equation to the data (Kaleidagraph, Synergy Software), as before (51).

2.8. Measurement of cell proliferation

Normal human melanocytes and dermal fibroblasts were isolated from the neonatal foreskin of African American donors following procedures previously described (31,52). Melanocytes were cultured in serum-free melanocyte basal medium (MBM-4) supplemented with melanocyte growth factors (MGM-4) (Lonza, Walkersville, MD). Fibroblasts were grown in Dulbecco's modified Eagle's medium (DMEM) supplemented with human FGF-basic, 10% charcoal-stripped fetal bovine serum (Serum Source International, Inc. Charlotte, NC) and 1% Antibiotic-Antimycotic Solution (Mediatech, Inc. Manassas, VA). To test the antiproliferative effect of the secosteroids, 200 cells were grown in 96 plates for 24 h followed by synchronization by growing in serum-free media for 24 h. Cells were treated with 20,25(OH)$_2$D3, 1,20,25(OH)$_3$D3, 20(OH)D3 or 1,25(OH)$_2$D3 for 72 h in the cell

culture medium and then the MTS (Promega, Madison, WI) assay was performed following the manufacturer's protocol.

2.9. Measurement of the interaction of secosteroids with RORα

RORα coactivator activities of secosteroids were determined using the The LanthaScreen TR-FRET RORα Coactivator kit, according to the manufacturer's instructions.

3. Results

3.1. Characterization of expressed CYP2R1

CYP2R1 was expressed in *E. coli* with the N-terminal transmembrane sequence deleted and a His_4 tag added to the C-terminus (41). To determine whether CYP2R1 was associated with the bacterial membranes, the distribution of CYP2R1 between the membrane and cytosol fractions of the *E.coli* cells was analyzed. SDS-PAGE revealed that a band that closely corresponds to the predicted mass of CYP2R1 (57.5 kDa) was present in the bacterial cells and in both the membrane and cytosol fractions (Fig. 1A). CO-reduced minus reduced difference spectra of the membrane and cytosol fractions (Fig. 1C and D, respectively) confirmed that there was P450 present in both fractions. For the cytosol the predominant peak was at 420 nm, representative of cytochrome P420 and/or bacterial cytochromes, and caused some inaccuracy in the quantitation of the P450 peak. The peak at 450 nm in the membrane fraction was notably larger than the 420 nm peak. Based on the peaks at 450 nm, 87.5% of total P450 was present in the membrane fraction showing that CYP2R1 interacts with the membrane despite the deletion of the N-terminal transmembrane sequence. To ensure that the maximal yield of CYP2R1 was achieved, CYP2R1 was purified from CHAPS extracts of whole *E. coli* cells rather than the membrane fraction.

Purification of CYP2R1 once by nickel-affinity chromatography removed the majority of unwanted proteins from the crude detergent extract (Fig. 1B), and the major band at 58.1 kDa was close to the predicted mass of CYP2R1 (57.5 kDa). Further purification by repeating the nickel-affinity chromatography removed most of the contaminating band at 67.4 kDa. A final purification step by hydrophobic-interaction chromatography using octyl-Sepharose largely removed remaining unwanted proteins. CYP2R1 was stable throughout the purification with minimal conversion to inactive cytochrome P420 (Fig. 1E), and the final yield of purified CYP2R1 was 361 nmol/L culture.

3.2. Metabolism of vitamin D3 by CYP2R1

We investigated three different assay systems for the addition of substrates to CYP2R1, via stock solutions in ethanol or 2-hydroxypropyl-β-cyclodextrin (HP-β-CD), or incorporated into the membrane of phospholipid vesicles, all previously used in assays of the activities of P450s (36,37,41,44,46,49–51,53). Vitamin D3 was metabolized to a single product in all three assay systems, identified as 25(OH)D3 (as expected) by comparison of its HPLC retention time to authentic standard. Addition of vitamin D3 from an ethanol stock, as employed in previous studies on CYP2R1 (40,41), displayed the highest conversion to 25(OH)D3, while addition from HP-β-CD displayed the lowest (Fig. 2A). Although conversion of vitamin D3 to 25(OH)D3 was lower from phospholipid vesicles compared to

ethanol, phospholipid vesicles were used to further characterize CYP2R1 as they mimic the natural environment of the P450 within the microsomal membrane, from which they access their hydrophobic substrate (42). Also, it is well-established that vitamin D and its hydroxylated products partition greater than 97% into the membrane of phospholipid vesicles (46,51,54). We examined the activity of CYP2R1 in vesicles of varying composition, including ones containing DOPC and cardiolipin as this system has been well-characterized and widely used for assaying other vitamin D-metabolizing P450 enzymes (44,46,49,51,54), and phosphatidylcholine and phosphatidylethanolamine, the two major phospholipids that constitute the microsomal membrane (55). The activity of CYP2R1 on vitamin D3 was not significantly different (ANOVA, $p>0.05$) between vesicles of all phospholipid compositions tested, including those made from saturated DMPC (Fig. 2B).

Cytochrome P450 oxidoreductase (POR) acts as the redox partner for microsomal P450 enzymes such as CYP2R1, delivering two electrons, one at a time (56). Therefore, we tested the effect of human POR on the ability of CYP2R1 to metabolize vitamin D3, and found that a concentration of 1 μM (ratio of 4:1 to CYP2R1), was required to achieve maximum activity (Fig. 2C). Similarly, cytochrome b_5 has been shown to serve as an alternative electron donor (57–59) for microsomal P450s such as CYP3A4, or as an allosteric modifier for CYP17A1 (60,61). Cytochrome b_5 is known to interact with the microsomal membrane (60), therefore we tested cytochrome b_5 concentrations that gave ratios to CYP2R1 of up to 3:1, in the presence of phospholipid vesicles. No significant effect was observed on the rate of vitamin D3 metabolism (ANOVA, $p>0.05$) (Fig. 2D) indicating that cytochrome b_5 is not a modulator of CYP2R1 activity.

3.3. Metabolism of 20(OH)D3 by CYP2R1

20(OH)D3, a product of CYP11A1 action on vitamin D3 present in serum, acts as a biased agonist on the VDR with low calcemic activity but strong effects on cell proliferation, differentiation and the immune system (see Introduction). We therefore tested the ability of CYP2R1 to metabolize this substrate. Incubation of 20(OH)D3 with CYP2R1 followed by extraction and analysis by HPLC showed formation of a single product (Fig. 3A, B). This product was identified as 20,25$(OH)_2$D3 by comparison of its retention time to authentic standard, followed by spiking with standard in a different HPLC solvent system (Fig. 3D – F). Comparison of the time course for metabolism of vitamin D3 and 20(OH)D3 by CYP2R1 revealed that both were approximately linear for 30 min, with 2.6-fold higher activity being seen with vitamin D3 at the substrate concentration used (Fig. 3C).

Another major metabolite produced by the action of CYP11A1 on vitamin D3, 20,23-dihydroxyvitamin D3 [20,23$(OH)_2$D3] (22,24), also displays biological activity (52,62), acting via nuclear receptors, VDR, RORα and RORγ (27). We therefore tested the ability of CYP2R1 to metabolize 20,23$(OH)_2$D3, however conversion to products was barely detectible (data not shown).

3.4. Comparison of kinetics for secosteroid metabolism by CYP2R1 and CYP27A1

CYP2R1 and CYP27A1 are known to hydroxylate vitamin D3 at C25, with the latter originally thought to be the major vitamin D 25-hydroxylase (63) before more recent genetic

studies implicated CYP2R1 as the major 25-hydroxylase (20,21). We therefore compared the ability of human CYP27A1 and CYP2R1 to metabolize vitamin D3 under identical conditions in a membrane environment. CYP2R1 converted vitamin D3 to 25(OH)D3 with a K_m of 0.017 mol/mol PL and a k_{cat} of 0.25 min^{-1} (Fig. 4A), while CYP27A1 metabolized vitamin D3 with a K_m of 0.65 mol/mol PL and k_{cat} of 0.56 min^{-1} (Fig. 4B). CYP2R1 therefore displays 17-fold higher catalytic efficiency (k_{cat}/K_m) as compared to CYP27A1 (14.7 mol PL.mol^{-1}.min^{-1} versus 0.86 mol PL.mol^{-1}.min^{-1}, respectively), due to its very much lower K_m in the membrane environment. As CYP2R1 also metabolizes 20(OH)D3 (Section 3.3), the kinetic parameters for the conversion of 20(OH)D3 to 20,25$(OH)_2$D3 were also examined. CYP2R1 displayed a K_m of 0.0026 mol/mol PL and k_{cat} of 0.035 min^{-1} (Fig. 4A). Both the K_m and k_{cat} for this conversion were lower than that for the hydroxylation of vitamin D3 so the overall catalytic efficiencies (k_{cat}/K_m) for these conversions, 13.4 versus 14.7 mol PL.mol^{-1}.min^{-1}, respectively, are similar.

3.5. Biological activity of 20,25$(OH)_2$D3

There are already some data indicating that the 20,25$(OH)_2$D3 product of CYP2R1 action on 20(OH)D3 retains activity, or displays even enhanced activity, compared to 20(OH)D3 (28,37). To further define the effect of 25-hydroxylation of 20(OH)D3 we compared the abilities of 20(OH)D3 and 20,25$(OH)_2$D3, as well as the CYP27B1-hydroxylation product 1,20,25$(OH)_3$D3, to inhibit the proliferation of melanocytes and dermal fibroblasts (Fig. 5). The 1α-hydroxy-derivative was included in this comparison as 20,25$(OH)_2$D3 is an excellent substrate for CYP27B1 (64) and 1,20,25$(OH)_3$D3 has been detected in human skin (39). 20,25$(OH)_2$D3 inhibited the proliferation of both melanocytes and dermal fibroblasts with IC_{50} values of 0.25×10^{-10} M and 0.45×10^{-10} M, respectively. Calculated IC_{50} values were somewhat lower than those for the parent 20(OH)D3. The potency of 20,25$(OH)_2$D3 was comparable to that of 1,25$(OH)_2$D3 for fibroblasts and melanocytes. The addition of a 1α-hydroxyl group to 20,25$(OH)_2$D3 had little effect on the IC_{50} values.

As well as evidence that 20(OH)D3 and 20,25$(OH)_2$D3 can act through binding to the VDR, there is recent evidence that they can also act as inverse agonists on RORα and RORγ (27–29). To further define this ability, we tested 20,25$(OH)_2$D3 in comparison to its parent 20(OH)D3 and to 1,25$(OH)_2$D3, to modulate coactivator peptide binding to RORα using the LanthaScreen TR-FRET RORα Coactivator kit. Agonists increase coactivator peptide binding and inverse agonists decrease coactivator peptide binding, with the binding being measured by time-resolved FRET. Results show that 20,25$(OH)_2$D3, 20(OH)D3 and 1,25$(OH)_2$D3 all decrease coactivator binding to RORα, with similar IC_{50} values (Fig. 6), indicating they act as inverse agonists, decreasing basal receptor activity.

4. Discussion

The initial 25-hydroxylation step of vitamin D3 activation is well-known to occur in the liver, with mitochondrial CYP27A1 originally thought to be the major P450 enzyme physiologically responsible for catalyzing this reaction (6,65). However, Cheng *et al.* identified the microsomal CYP2R1 from screening a cDNA library prepared from CYP27A1-deficient mice and demonstrated that it displayed vitamin D 25-hydroxylase

activity (19). Genetic analyses of patients presenting with vitamin D deficiency in the form of skeletal abnormalities, hypocalcemia and hypophosphatemia, revealed that a Leu99Pro mutation in the CYP2R1 gene was common in all three patients (20,21). This, plus the observation that CYP27A1 mutations do not cause symptoms of vitamin D deficiency (17,66), indicate that CYP2R1 is the physiologically important vitamin D 25-hydroxylase. In our study, we compared the ability of purified CYP2R1 and CYP27A1 to metabolize vitamin D3 in an identical system of phospholipid vesicles. This revealed that CYP2R1 had a k_{cat} half that of CYP27A1 but a K_m 38-times lower, giving CYP2R1 a 17-fold higher catalytic efficiency over CYP27A1 for 25-hydroxylation of vitamin D3, consistent with it being the major 25-hydroxylase. This is also in general agreement with another study where a comparison of activities was done under non-identical conditions (40). It should also be noted that CYP27A1 acts on cholesterol and bile acids such as 5β-cholestane-3α,7α,12α-triol in the liver (67). These are preferred substrates that will efficiently compete with vitamin D3 for binding to the enzyme, further reducing its ability to produce 25(OH)D3. In contrast, CYP2R1 has high substrate specificity with only vitamins D2 and D3 (and 20(OH)D3 as discussed below) as known endogenous substrates (40,41). As CYP27A1 is expressed in various tissues other than liver, such as the skin (66,68), it may contribute to local production of 25(OH)D3 at these sites, where bile acid synthesis does not occur.

Mammalian cytochromes P450 are membrane-bound proteins with their catalytic domains open to the hydrophobic region of the phospholipid membrane from which they access hydrophobic substrates such as vitamin D (41,42,45). Microsomal P450s have a transmembrane anchor at the N-terminus plus a second site of hydrophobic binding primarily involving the A′-, F′-, and G′-helices and the F-G loop, at the perimeter of the substrate access channel (42). The CYP2R1 used in our study and another (41) has the N-terminal domain deleted but our results show that it is still predominantly associated with the bacterial membrane fraction, presumably by this second site (41). Consistent with this, our study shows that the CYP2R1 construct can use vitamin D3 within the membrane of phospholipid vesicles, with good adherence to Michaelis-Menten kinetics. While we cannot exclude that the activity of the CYP2R1 on vesicle-associated substrate is influenced by the lack of the N-terminal anchor, the vesicle system does provide a model that can be experimentally manipulated, that resembles the endoplasmic reticulum. Such a model has been used extensively with mitochondrial P450s which do not have an N-terminal membrane anchor (44,46,49,51,53,54,68). It should be noted that it has previously been shown that vitamin D and its hydroxy-derivatives strongly partition (>97%) into the membrane of phospholipid vesicles (46,51,54), thus providing a direct source of substrate to the access channel of the P450.

The phospholipid vesicles primarily used in this study comprised DOPC and cardiolipin, extensively employed in the study of mitochondrial P450s that metabolize various forms of vitamin D (44,46,49,51,53,54,68). Unlike mitochondrial P450s such as CYP11A1 (69) and CYP27B1 (49) where the phospholipid composition markedly influenced catalytic activity, varying the phospholipid composition of vesicles had little effect on CYP2R1 activity. Activities were similar in membranes resembling microsomes (DOPC and DOPE) (55), or resembling mitochondria (DOPC and cardiolipin), or with completely saturated acyl chains (DMPC). This may reflect a less hydrophobic interaction between the CYP2R1 construct

and the membrane than seen for mitochondrial P450s, the latter having a longer F-G loop (70).

Microsomal P450s require electrons transferred via NADPH-P450 oxidoreductase (POR) and it has previously been shown that POR deficiency results in dysfunctional steroidogenesis (71). Our study is the first to use human POR to support CYP2R1 activity in a reconstituted system and we found that a concentration of 1.0 μM was sufficient to saturate the CYP2R1, and corresponded to a POR to CYP2R1 ratio of 4:1. Cytochrome b_5, which is also associated with the microsomal membrane, can deliver electrons to some P450 enzymes, in conjunction with or as an alternative to POR (60,71). In some instances, rather than deliver electrons it acts as an allosteric modifier, such as for 17,20-lyase activity by CYP17A1 (60,61). We added cytochrome b_5 to CYP2R1 at ratios of up to 3:1, but no effect on activity was observed. This is consistent with a previous report on CYP2R1 metabolism of vitamin D3 carried out in the absence of a membrane and without human POR (41).

We have previously reported that 20,25$(OH)_2$D3 is present in human skin and serum, indicating its *in vivo* production (39). Our study shows that CYP2R1 can produce this product from 20(OH)D3. Besides CYP2R1, other vitamin D metabolizing P450s, CYP27A1, CYP24A1 and CYP3A4, can also metabolize 20(OH)D3 to 20,25$(OH)_2$D3. Unlike CYP2R1 they make a range of other products as well including both C24 stereoisomers of 20,24$(OH)_2$D3 for CYP24A1 and CYP3A4, and 20,26$(OH)_2$D3 for CYP27A1 (36,37,44,53). CYP2R1 displays a K_m for 20(OH)D3 12-fold lower than any of these other CYPs that convert 20(OH)D3 to 20,25$(OH)_2$D3 and may therefore be the most important *in vivo*, where 20(OH)D3 concentrations are low compared to D3 and 25(OH)D3 (39). It should be noted that 25(OH)D3 is not a substrate for CYP11A1, so 20,25$(OH)_2$D3 cannot be made from 25(OH)D3 (24).

It has previously been shown that 20,25$(OH)_2$D3 can reduce colony formation by SKMEL-188 melnoma cells in soft agar, with this inhibition being significantly greater than that caused by either 20(OH)D3 or 1,25$(OH)_2$D3 at a concentration of 0.1 nM (37). It has also been shown to inhibit keratinocyte proliferation with a similar IC_{50} to 1,25$(OH)_2$D3. It stimulated the movement of a VDR-GFP construct from the cytoplasm to the nucleus of melanoma cells with high potency ($EC_{50} = 6 \times 10^{-10}$ M), providing strong evidence that it can act via the VDR and supporting molecular modelling studies which predict its high affinity binding to the VDR (28). The current study further shows that 20,25$(OH)_2$D3 displays potency at least as good, if not better than that of its parent 20(OH)D3 for inhibiting the proliferation of both melanocytes and dermal fibroblasts. The potency of 20,25$(OH)_2$D3 was similar to that of 1,25$(OH)_2$D3. The addition of a 1α-hydroxyl group to 20,25$(OH)_2$D3, a reaction efficiently catalyzed by CYP27B1, had little effect on the potency for inhibition of proliferation, as seen previously for inhibition of colony formation by melanoma cells (64).

RORα, and RORγ are found in various tissues including the skin, display basal activity in the absence of ligand, and regulate metabolism and the immune system, including transcription of the IL-17 gene (27,72). Natural ligands include sterols and oxysterols, some acting as agonists, others as inverse agonists. Recently CYP11A1-derived 20(OH)D3 and 20,23$(OH)_2$D3 have been identified as inverse agonists of RORα and RORγ (27,72).

Molecular modelling studies predict that 20,25(OH)$_2$D3 also binds to RORα, and RORγ. There is some experimental evidence for this with 20,25(OH)$_2$D3 inhibiting ROR-luciferase reporter activity in HaCat keratinocytes with an IC_{50} of 7×10^{-10} M, slightly higher than for 20(OH)D3 or 1,25(OH)$_2$D3 (28). The present work further shows that 20,25(OH)$_2$D3 can inhibit coactivator binding to RORα, confirming that it acts as an inverse agonist, with similar potency to the parent 20(OH)D3 and to 1,25(OH)$_2$D3. Thus, overall it appears that hydroxylation of 20(OH)D3 by CYP2R1, (or by other vitamin D3-metabolizing P450s) maintains or enhances the VDR-mediated effects of the secosteroid, and does not alter its ability to interact with RORα.

Acknowledgments

We would like to acknowledge The University of Western Australia and the Research Training Program for their financial support to CYSC. The work was supported in part by grants from the National Institutes of Health (R21AR066505-01A1, 1R01AR071189-01A1 and 1R01AR056666-01A2) to ATS.

Abbreviations

1,25(OH)$_2$D3	1α,25-dihydroxyvitamin D3
25(OH)D3	25-hydroxyvitamin D3
20(OH)D3	20*S*-hydroxyvitamin D3
20,25(OH)$_2$D3	20*S*,25-dihydroxyvitamin D3
20,23(OH)$_2$D3	20*S*,23*S*-dihydroxyvitamin D3
1,20,25(OH)$_3$D3	1α,20*S*,25-trihydroxyvitamin D3
CYP	cytochrome P450
DOPC	dioleoyl phosphatidylcholine
DOPE	dioleoyl phosphatidylethanolamine
DMPC	dimyristoyl phosphatidylcholine
HP-β-CD	2-hydroxypropyl-β-cyclodextrin
PL	phospholipid
POR	NADPH-P450 oxidoreductase
RORα	retinoic acid-related orphan receptor α
RORγ	retinoic acid-related orphan receptor γ

References

1. Holick MF. Vitamin D: A millenium perspective. J Cell Biochem. 2003; 88:296–307. [PubMed: 12520530]
2. Henry, HL. Comprehensive Physiology. John Wiley & Sons, Inc; 2010. Vitamin D; p. 699-718.

3. Bikle DD. Vitamin D metabolism, mechanism of action, and clinical applications. Chem Biol. 2014; 21:319–329. [PubMed: 24529992]
4. Christakos S, Hewison M, Gardner DG, Wagner CL, Sergeev IN, Rutten E, Pittas AG, Boland R, Ferrucci L, Bikle DD. Vitamin D: beyond bone. Ann N Y Acad Sci. 2013; 1287:45–58. [PubMed: 23682710]
5. DeLuca HF. Overview of general physiologic features and functions of vitamin D. Am J Clin Nutr. 2004; 80:1689S–1696S. [PubMed: 15585789]
6. Jones G, Strugnell SA, DeLuca HF. Current understanding of the molecular actions of vitamin D. Physiol Rev. 1998; 78:1193–1231. [PubMed: 9790574]
7. Pike JW, Meyer MB. The vitamin D receptor: new paradigms for the regulation of gene expression by 1,25-dihydroxyvitamin D3. Rheum Dis Clin North Am. 2012; 38:13–27. [PubMed: 22525840]
8. Carlberg C. Molecular basis of the selective activity of vitamin D analogues. J Cell Biochem. 2003; 88:274–281. [PubMed: 12520526]
9. Boland RL. VDR activation of intracellular signaling pathways in skeletal muscle. Mol Cell Endocrinol. 2011; 347:11–16. [PubMed: 21664245]
10. Haussler MR, Jurutka PW, Mizwicki M, Norman AW. Vitamin D receptor (VDR)-mediated actions of 1α,25(OH)2vitamin D3: Genomic and non-genomic mechanisms. Best Pract Res Cl En. 2011; 25:543–559.
11. DeLuca HF. The vitamin D story: a collaborative effort of basic science and clinical medicine. Faseb j. 1988; 2:224–236. [PubMed: 3280376]
12. Schuster I. Cytochromes P450 are essential players in the vitamin D signaling system. Biochim Biophys Acta. 2011; 1814:186–199. [PubMed: 20619365]
13. Bjorkhem I, Holmberg I. Assay and properties of a mitochondrial 25-hydroxylase active on vitamine D3. J Biol Chem. 1978; 253:842–849. [PubMed: 23383]
14. Ohyama Y, Masumoto O, Usui E, Okuda K. Multi-functional property of rat liver mitochondrial cytochrome P-450. J Biochem. 1991; 109:389–393. [PubMed: 1880123]
15. Hayashi S, Noshiro M, Okuda K. Isolation of a cytochrome P-450 that catalyzes the 25-hydroxylation of vitamin D3 from rat liver microsomes. J Biochem. 1986; 99:1753–1763. [PubMed: 3745145]
16. Madhok TC, DeLuca HF. Characteristics of the rat liver microsomal enzyme system converting cholecalciferol into 25-hydroxycholecalciferol. Evidence for the participation of cytochrome p-450. Biochem J. 1979; 184:491–499. [PubMed: 231972]
17. Rosen H, Reshef A, Maeda N, Lippoldt A, Shpizen S, Triger L, Eggertsen G, Bjorkhem I, Leitersdorf E. Markedly reduced bile acid synthesis but maintained levels of cholesterol and vitamin D metabolites in mice with disrupted sterol 27-hydroxylase gene. J Biol Chem. 1998; 273:14805–14812. [PubMed: 9614081]
18. Okuda KI. Liver mitochondrial P450 involved in cholesterol catabolism and vitamin D activation. J Lipid Res. 1994; 35:361–372. [PubMed: 8014573]
19. Cheng JB, Motola DL, Mangelsdorf DJ, Russell DW. Deorphanization of cytochrome P450 2R1: a microsomal vitamin D 25-hydroxylase. J Biol Chem. 2003; 278:38084–38093. [PubMed: 12867411]
20. Cheng JB, Levine MA, Bell NH, Mangelsdorf DJ, Russell DW. Genetic evidence that the human CYP2R1 enzyme is a key vitamin D 25-hydroxylase. P Natl Acad Sci USA. 2004; 101:7711–7715.
21. Al Mutair AN, Nasrat GH, Russell DW. Mutation of the CYP2R1 vitamin D 25-hydroxylase in a Saudi Arabian family with severe vitamin D deficiency. J Clin Endocrinol Metab. 2012; 97:E2022–2025. [PubMed: 22855339]
22. Tuckey RC, Li W, Zjawiony JK, Zmijewski MA, Nguyen MN, Sweatman T, Miller D, Slominski A. Pathways and products for the metabolism of vitamin D3 by cytochrome P450scc. FEBS J. 2008; 275:2585–2596. [PubMed: 18410379]
23. Guryev O, Carvalho RA, Usanov S, Gilep A, Estabrook RW. A pathway for the metabolism of vitamin D3: unique hydroxylated metabolites formed during catalysis with cytochrome P450scc (CYP11A1). Proc Natl Acad Sci U S A. 2003; 100:14754–14759. [PubMed: 14657394]

24. Slominski A, Semak I, Zjawiony J, Wortsman J, Li W, Szczesniewski A, Tuckey RC. The cytochrome P450scc system opens an alternate pathway of vitamin D3 metabolism. FEBS J. 2005; 272:4080–4090. [PubMed: 16098191]
25. Slominski AT, Kim TK, Shehabi HZ, Semak I, Tang EKY, Nguyen MN, Benson HAE, Korik E, Janjetovic Z, Chen J, Yates CR, Postlethwaite A, Li W, Tuckey RC. In vivo evidence for a novel pathway of vitamin D3 metabolism initiated by P450scc and modified by CYP27B1. FASEB J. 2012; 26:3901–3915. [PubMed: 22683847]
26. Tuckey RC, Li W, Shehabi HZ, Janjetovic Z, Nguyen MN, Kim TK, Chen J, Howell DE, Benson HAE, Sweatman T, Baldisseri DM, Slominski A. Production of 22-hydroxy metabolites of vitamin D3 by cytochrome P450scc (CYP11A1) and analysis of their biological activities on skin cells. Drug Metab Dispos. 2011; 39:1577–1588. [PubMed: 21677063]
27. Slominski AT, Kim TK, Takeda Y, Janjetovic Z, Brozyna AA, Skobowiat C, Wang J, Postlethwaite A, Li W, Tuckey RC, Jetten AM. RORalpha and ROR gamma are expressed in human skin and serve as receptors for endogenously produced noncalcemic 20-hydroxy- and 20,23-dihydroxyvitamin D. FASEB J. 2014; 28:2775–2789. [PubMed: 24668754]
28. Slominski AT, Kim TK, Hobrath JV, Oak AS, Tang EK, Tieu EW, Li W, Tuckey RC, Jetten AM. Endogenously produced nonclassical vitamin D hydroxy-metabolites act as “biased” agonists on VDR and inverse agonists on RORalpha and RORgamma. J Steroid Biochem Mol Biol. 2016; doi: 10.1016/j.jsbmb.2016.1009.1024
29. Slominski AT, Kim TK, Li W, Yi AK, Postlethwaite A, Tuckey RC. The role of CYP11A1 in the production of vitamin D metabolites and their role in the regulation of epidermal functions. J Steroid Biochem Mol Biol. 2014; 144 Pt A:28–39. [PubMed: 24176765]
30. Wang J, Slominski A, Tuckey RC, Janjetovic Z, Kulkarni A, Chen J, Postlethwaite AE, Miller D, Li W. 20-Hydroxyvitamin D3 inhibits proliferation of cancer cells with high efficacy while being non-toxic. Anticancer Res. 2012; 32:739–746. [PubMed: 22399586]
31. Janjetovic Z, Zmijewski MA, Tuckey RC, DeLeon DA, Nguyen MN, Pfeffer LM, Slominski AT. 20-Hydroxycholecalciferol, product of vitamin D3 hydroxylation by P450scc, decreases NF-κB activity by increasing IκBα levels in human keratinocytes. PLoS ONE. 2009; 4:e5988. [PubMed: 19543524]
32. Zbytek B, Janjetovic Z, Tuckey RC, Zmijewski MA, Sweatman TW, Jones E, Nguyen MN, Slominski AT. 20-Hydroxyvitamin D3, a product of vitamin D3 hydroxylation by cytochrome P450scc, stimulates keratinocyte differentiation. J Invest Dermatol. 2008; 128:2271–2280. [PubMed: 18368131]
33. Slominski AT, Janjetovic Z, Fuller BE, Zmijewski MA, Tuckey RC, Nguyen MN, Sweatman T, Li W, Zjawiony J, Miller D, Chen TC, Lozanski G, Holick MF. Products of vitamin D3 or 7-dehydrocholesterol metabolism by cytochrome P450scc show anti-leukemia effects, having low or absent calcemic activity. PLoS ONE. 2010; 5:e9907. [PubMed: 20360850]
34. Slominski AT, Manna PR, Tuckey RC. On the role of skin in the regulation of local and systemic steroidogenic activities. Steroids. 2015; 103:72–88. [PubMed: 25988614]
35. Gupta RP, Hollis BW, Patel SB, Patrick KS, Bell NH. CYP3A4 is a human microsomal vitamin D 25-hydroxylase. J Bone Miner Res. 2004; 19:680–688. [PubMed: 15005856]
36. Cheng CY, Slominski AT, Tuckey RC. Hydroxylation of 20-hydroxyvitamin D3 by human CYP3A4. J Steroid Biochem Mol Biol. 2016; 159:131–141. [PubMed: 26970587]
37. Tieu EW, Tang EKY, Chen J, Li W, Nguyen MN, Janjetovic Z, Slominski A, Tuckey RC. Rat CYP24A1 acts on 20-hydroxyvitamin D3 producing hydroxylated products with increased biological activity. Biochem Pharmacol. 2012; 84:1696–1704. [PubMed: 23041230]
38. Lin Z, Marepally SR, Ma D, Myers LK, Postlethwaite AE, Tuckey RC, Cheng CY, Kim TK, Yue J, Slominski AT, Miller DD, Li W. Chemical Synthesis and Biological Activities of 20S,24S/R-Dihydroxyvitamin D3 Epimers and Their 1alpha-Hydroxyl Derivatives. J Med Chem. 2015; 58:7881–7887. [PubMed: 26367019]
39. Slominski AT, Kim TK, Li W, Postlethwaite A, Tieu EW, Tang EK, Tuckey RC. Detection of novel CYP11A1-derived secosteroids in the human epidermis and serum and pig adrenal gland. Sci Rep. 2015; 5:14875. [PubMed: 26445902]

40. Shinkyo R, Sakaki T, Kamakura M, Ohta M, Inouye K. Metabolism of vitamin D by human microsomal CYP2R1. Biochem Bioph Res Co. 2004; 324:451–457.
41. Strushkevich N, Usanov SA, Plotnikov AN, Jones G, Park HW. Structural Analysis of CYP2R1 in Complex with Vitamin D3. J Mol Biol. 2008; 380:95–106. [PubMed: 18511070]
42. Berka K, Paloncyova M, Anzenbacher P, Otyepka M. Behavior of human cytochromes P450 on lipid membranes. J Phys Chem B. 2013; 117:11556–11564. [PubMed: 23987570]
43. Parikh A, Gillam EM, Guengerich FP. Drug metabolism by Escherichia coli expressing human cytochromes P450. Nat Biotechnol. 1997; 15:784–788. [PubMed: 9255795]
44. Tieu EW, Li W, Chen J, Baldisseri DM, Slominski AT, Tuckey RC. Metabolism of cholesterol, vitamin D3 and 20-hydroxyvitamin D3 incorporated into phospholipid vesicles by human CYP27A1. J Steroid Biochem. 2012; 129:163–171.
45. Strushkevich N, MacKenzie F, Cherkesova T, Grabovec I, Usanov S, Park HW. Structural basis for pregnenolone biosynthesis by the mitochondrial monooxygenase system. P Natl Acad Sci USA. 2011; 108:10139–10143.
46. Tang EK, Voo KJ, Nguyen MN, Tuckey RC. Metabolism of substrates incorporated into phospholipid vesicles by mouse 25-hydroxyvitamin D3 1alpha-hydroxylase (CYP27B1). J Steroid Biochem Mol Biol. 2010; 119:171–179. [PubMed: 20193763]
47. Bonina TA, Gilep AA, Estabrook RW, Usanov SA. Engineering of proteolytically stable NADPH-cytochrome P450 reductase. Biochemistry (Mosc). 2005; 70:357–365. [PubMed: 15823091]
48. Pesce MA, Strande CS. A new micromethod for determination of protein in cerebrospinal fluid and urine. Clin Chem. 1973; 19:1265–1267. [PubMed: 4128002]
49. Tang EK, Tieu EW, Tuckey RC. Expression of human CYP27B1 in Escherichia coli and characterization in phospholipid vesicles. Febs j. 2012; 279:3749–3761. [PubMed: 22862690]
50. Tuckey RC, Kamin H. Kinetics of the incorporation of adrenal cytochrome P-450scc into phosphatidylcholine vesicles. J Biol Chem. 1982; 257:2887–2893. [PubMed: 7061453]
51. Tuckey RC, Nguyen MN, Slominski A. Kinetics of vitamin D3 metabolism by cytochrome P450scc (CYP11A1) in phospholipid vesicles and cyclodextrin. Int J Biochem Cell Biol. 2008; 40:2619–2626. [PubMed: 18573681]
52. Janjetovic Z, Tuckey RC, Nguyen MN, Thorpe EM Jr, Slominski AT. 20,23-dihydroxyvitamin D3, novel P450scc product, stimulates differentiation and inhibits proliferation and NF-kappaB activity in human keratinocytes. J Cell Physiol. 2010; 223:36–48. [PubMed: 20020487]
53. Tieu EW, Li W, Chen J, Kim TK, Ma D, Slominski AT, Tuckey RC. Metabolism of 20-hydroxyvitamin D3 and 20,23-dihydroxyvitamin D3 by rat and human CYP24A1. J Steroid Biochem Mol Biol. 2015; 149:153–165. [PubMed: 25727742]
54. Tieu EW, Tang EK, Tuckey RC. Kinetic analysis of human CYP24A1 metabolism of vitamin D via the C24-oxidation pathway. FEBS J. 2014; 281:3280–3296. [PubMed: 24893882]
55. Davison SC, Wills ED. Studies on the lipid composition of the rat liver endoplasmic reticulum after induction with phenobarbitone and 20-methylcholanthrene. Biochem J. 1974; 140:461–468. [PubMed: 4447625]
56. Im SC, Waskell L. The interaction of microsomal cytochrome P450 2B4 with its redox partners, cytochrome P450 reductase and cytochrome b(5). Arch Biochem Biophys. 2011; 507:144–153. [PubMed: 21055385]
57. Schenkman JB, Jansson I. The many roles of cytochrome b5. Pharmacol Ther. 2003; 97:139–152. [PubMed: 12559387]
58. Hildebrandt A, Estabrook RW. Evidence for the participation of cytochrome b 5 in hepatic microsomal mixed-function oxidation reactions. Arch Biochem Biophys. 1971; 143:66–79. [PubMed: 4397839]
59. Oshino N, Imai Y, Sato R. A function of cytochrome b5 in fatty acid desaturation by rat liver microsomes. J Biochem. 1971; 69:155–167. [PubMed: 5543646]
60. Storbeck KH, Swart AC, Goosen P, Swart P. Cytochrome b5: novel roles in steroidogenesis. Mol Cell Endocrinol. 2013; 371:87–99. [PubMed: 23228600]
61. Miller WL. The syndrome of 17,20 lyase deficiency. J Clin Endocrinol Metab. 2012; 97:59–67. [PubMed: 22072737]

62. Kim TK, Wang J, Janjetovic Z, Chen J, Tuckey RC, Nguyen MN, Tang EKY, Miller D, Li W, Slominski AT. Correlation between secosteroid-induced vitamin D receptor activity in melanoma cells and computer-modeled receptor binding strength. Mol Cell Endocrinol. 2012; 361:143–152. [PubMed: 22546549]

63. Zhu J, DeLuca HF. Vitamin D 25-hydroxylase – Four decades of searching, are we there yet? Arch Biochem Biophys. 2012; 523:30–36. [PubMed: 22310641]

64. Tang EK, Chen J, Janjetovic Z, Tieu EW, Slominski AT, Li W, Tuckey RC. Hydroxylation of CYP11A1-derived products of vitamin D3 metabolism by human and mouse CYP27B1. Drug Metab Dispos. 2013; 41:1112–1124. [PubMed: 23454830]

65. Guo YD, Strugnell S, Back DW, Jones G. Transfected human liver cytochrome P-450 hydroxylates vitamin D analogs at different side-chain positions. P Natl Acad Sci USA. 1993; 90:8668–8672.

66. Skrede S, Bjorkhem I, Kvittingen EA, Buchmann MS, Lie SO, East C, Grundy S. Demonstration of 26-hydroxylation of C27-steroids in human skin fibroblasts, and a deficiency of this activity in cerebrotendinous xanthomatosis. J Clin Invest. 1986; 78:729–735. [PubMed: 3745434]

67. Pikuleva IA, Babiker A, Waterman MR, Bjorkhem I. Activities of recombinant human cytochrome P450c27 (CYP27) which produce intermediates of alternative bile acid biosynthetic pathways. J Biol Chem. 1998; 273:18153–18160. [PubMed: 9660774]

68. Vantieghem K, Overbergh L, Carmeliet G, De Haes P, Bouillon R, Segaert S. UVB-induced 1,25(OH)2D3 production and vitamin D activity in intestinal CaCo-2 cells and in THP-1 macrophages pretreated with a sterol Delta7-reductase inhibitor. J Cell Biochem. 2006; 99:229–240. [PubMed: 16598763]

69. Lambeth JD, Kitchen SE, Farooqui AA, Tuckey R, Kamin H. Cytochrome P-450scc-substrate interactions. Studies of binding and catalytic activity using hydroxycholesterols. J Biol Chem. 1982; 257:1876–1884. [PubMed: 7056749]

70. Headlam MJ, Wilce MCJ, Tuckey RC. The F–G loop region of cytochrome P450scc (CYP11A1) interacts with the phospholipid membrane. Biochim Biophys Acta. 2003; 1617:96–108. [PubMed: 14637024]

71. Riddick DS, Ding X, Wolf CR, Porter TD, Pandey AV, Zhang QY, Gu J, Finn RD, Ronseaux S, McLaughlin LA, Henderson CJ, Zou L, Fluck CE. NADPH-cytochrome P450 oxidoreductase: roles in physiology, pharmacology, and toxicology. Drug Metab Dispos. 2013; 41:12–23. [PubMed: 23086197]

72. Slominski AT, Brozyna AA, Zmijewski MA, Jozwicki W, Jetten AM, Mason RS, Tuckey RC, Elmets CA. Vitamin D signaling and melanoma: role of vitamin D and its receptors in melanoma progression and management. Lab Invest. 2017; 97:706–724. [PubMed: 28218743]

Highlights

- Purified CYP2R1 can convert membrane-associated vitamin D3 to 25(OH)D3
- CYP2R1 metabolizes vitamin D3 with 17-fold higher catalytic efficiency than CYP27A1
- CYP2R1 acts on 20(OH)D3 producing 20,25$(OH)_2$D3
- CYP2R1 shows similar catalytic efficiency for metabolism of 20(OH)D3 and vitamin D3
- 20,25$(OH)_2$D3 retains the biological activity of the parent 20(OH)D3

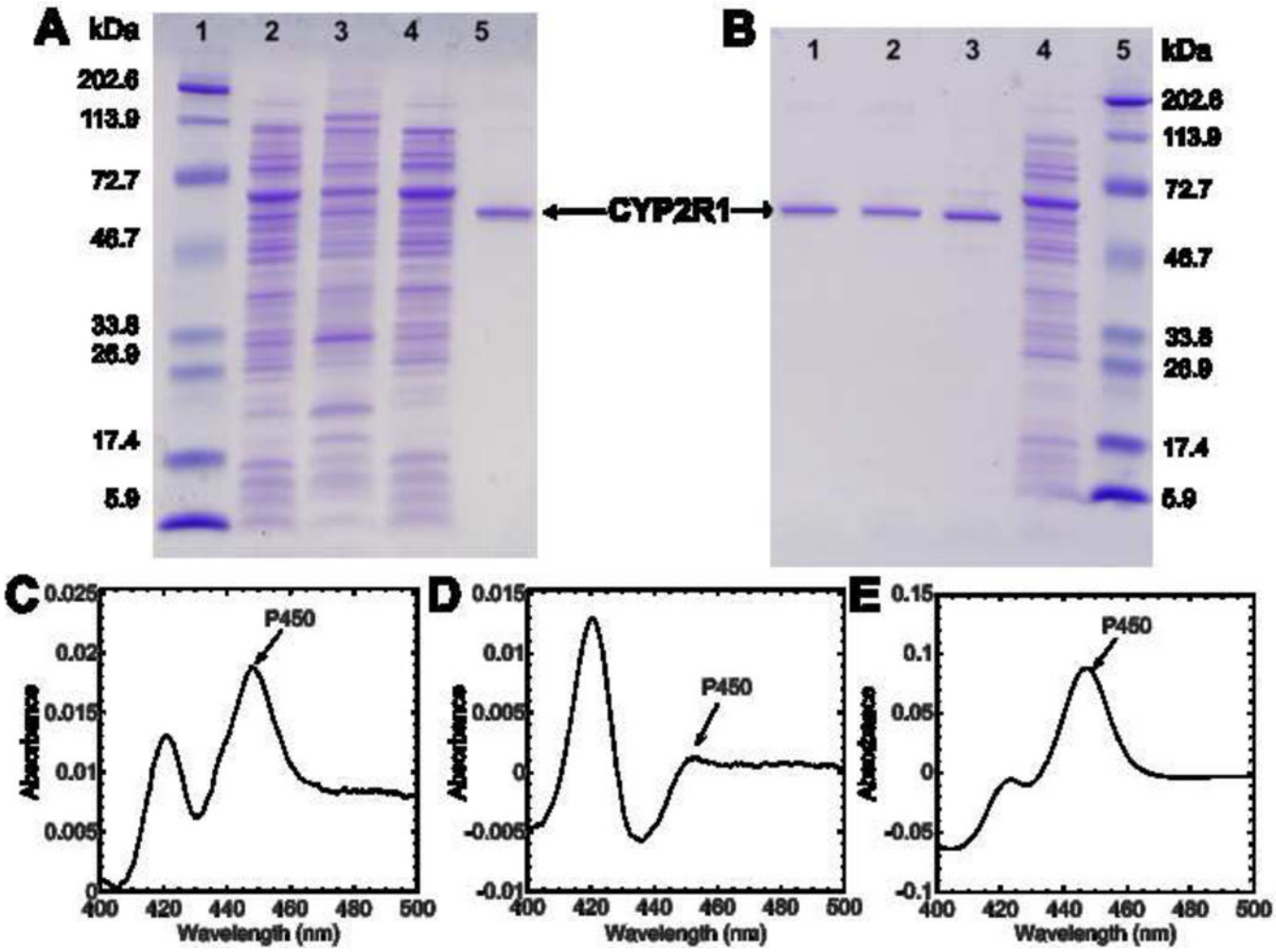

Fig. 1.

SDS-PAGE analysis and difference spectra for CYP2R1 expression and purification. (A) SDS-PAGE analysis of the membrane and cytosol fractions of *E. coli*. Lane 1: Molecular weight markers. Lane 2: Resuspended cell pellet (5 μg). Lane 3: Membrane fraction (5 μg). Lane 4: Cytosol fraction (5 μg). Lane 5: CYP2R1 purified twice by Ni-affinity chromatography, followed by hydrophobic chromatography on octyl-Sepharose. (B) SDS-PAGE analysis of the CYP2R1 purification. Lane 1: CYP2R1 (0.25 μg) purified twice by Ni-affinity chromatography, followed once by hydrophobic chromatography on octyl-Sepharose. Lane 2: CYP2R1 (0.25 μg) purified twice by Ni-affinity chromatography. Lane 3: CYP2R1(0.25 μg) purified once by Ni-affinity chromatography. Lane 4: *E. coli* cell CHAPS extract (2.5 μg) before purification. Lane 5: Molecular weight markers. (C) Reduced CO-minus reduced difference spectrum of the membrane fraction (see section 2.2). (D) Reduced CO-minus reduced difference spectrum of the cytosol fraction (see section 2.2). (E) Reduced CO-minus reduced difference spectrum of the final purified CYP2R1.

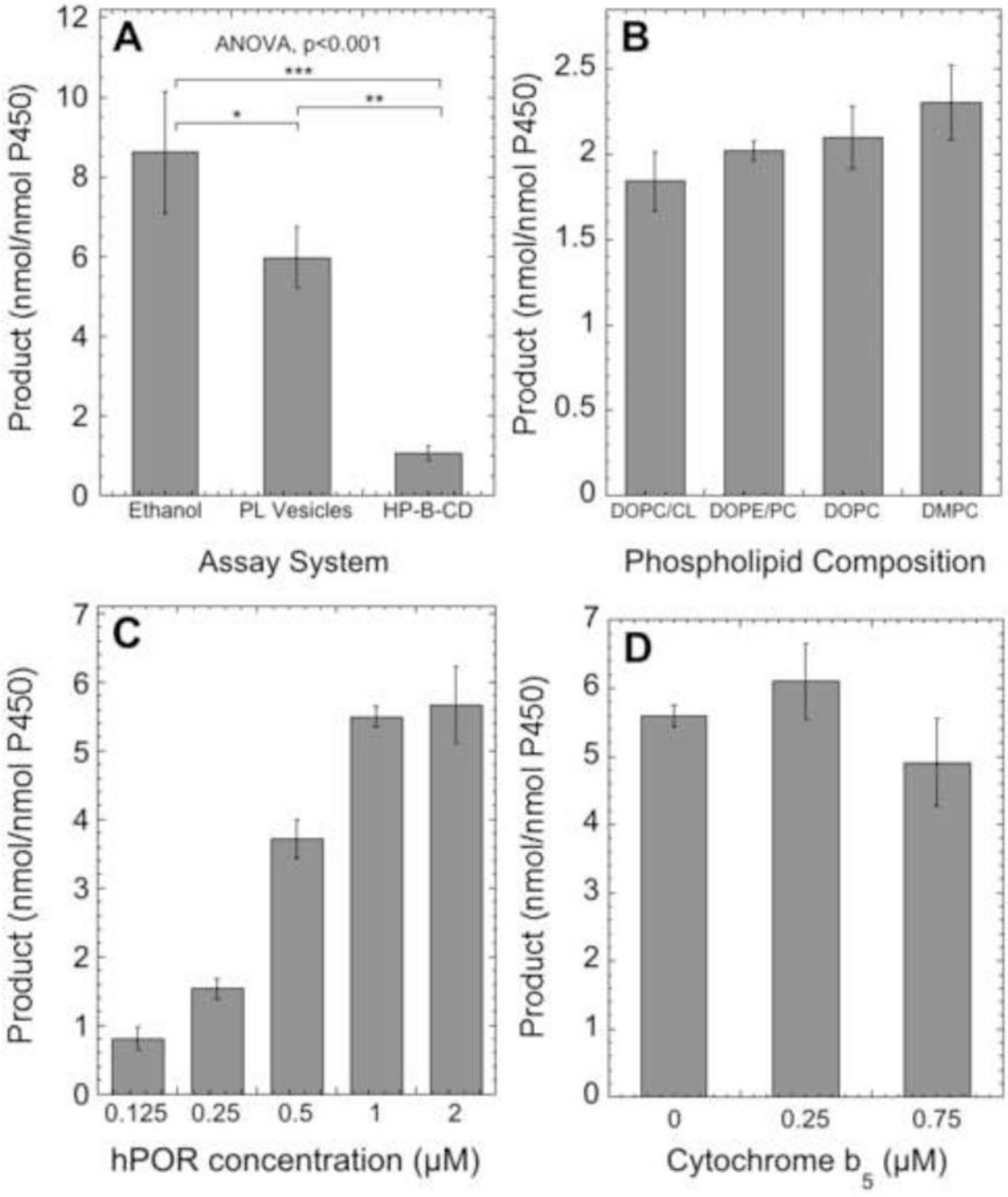

Fig. 2.

The effect of the assay system, phospholipid composition, human POR concentration and cytochrome b_5 on CYP2R1 activity. Incubations were carried out with 0.25 μM CYP2R1 at 37°C, and products were extracted and analyzed by reverse-phase HPLC using a 64 – 100% methanol in water gradient for 15 min, then 100% methanol for 40 min. Data are presented as mean ± SD for three replicates. (A) Comparison of reconstituted assay systems for CYP2R1. Vitamin D3 was added from a stock ethanol solution to a final concentration of 50 μM (2% ethanol) or added from a stock of 4.5% HP-β-CD to a final concentration of 50 μM

(0.45% HP-β-CD), or incorporated into phospholipid vesicles (510 μM phospholipid, 0.1 mol/mol PL). Incubations were carried out for 40 min with 1.0 μM POR. The statistical significance of differences were evaluated by Tukey's HSD test where *$p<0.05$, **$p<0.01$, ***$p<0.001$, and one-way ANOVA as shown on the panel. (B) Effect of phospholipid composition on CYP2R1 activity. Vitamin D3 was incorporated into vesicles of differing compositions (section 2.5) and incubated with CYP2R1 for 30 min with 1.0 μM POR. (C) Effect of POR concentration on CYP2R1 activity. The reactions with vitamin D3 in vesicles (0.04 mol/mol PL) were started with various concentrations of POR and carried out for 30 min. (D) Effect of cytochrome b_5 on CYP2R1 activity. The reactions with vitamin D3 (0.1 mol/mol PL) were started with POR (1.0 μM) in the presence or absence of cytochrome b_5, and carried out for 30 min.

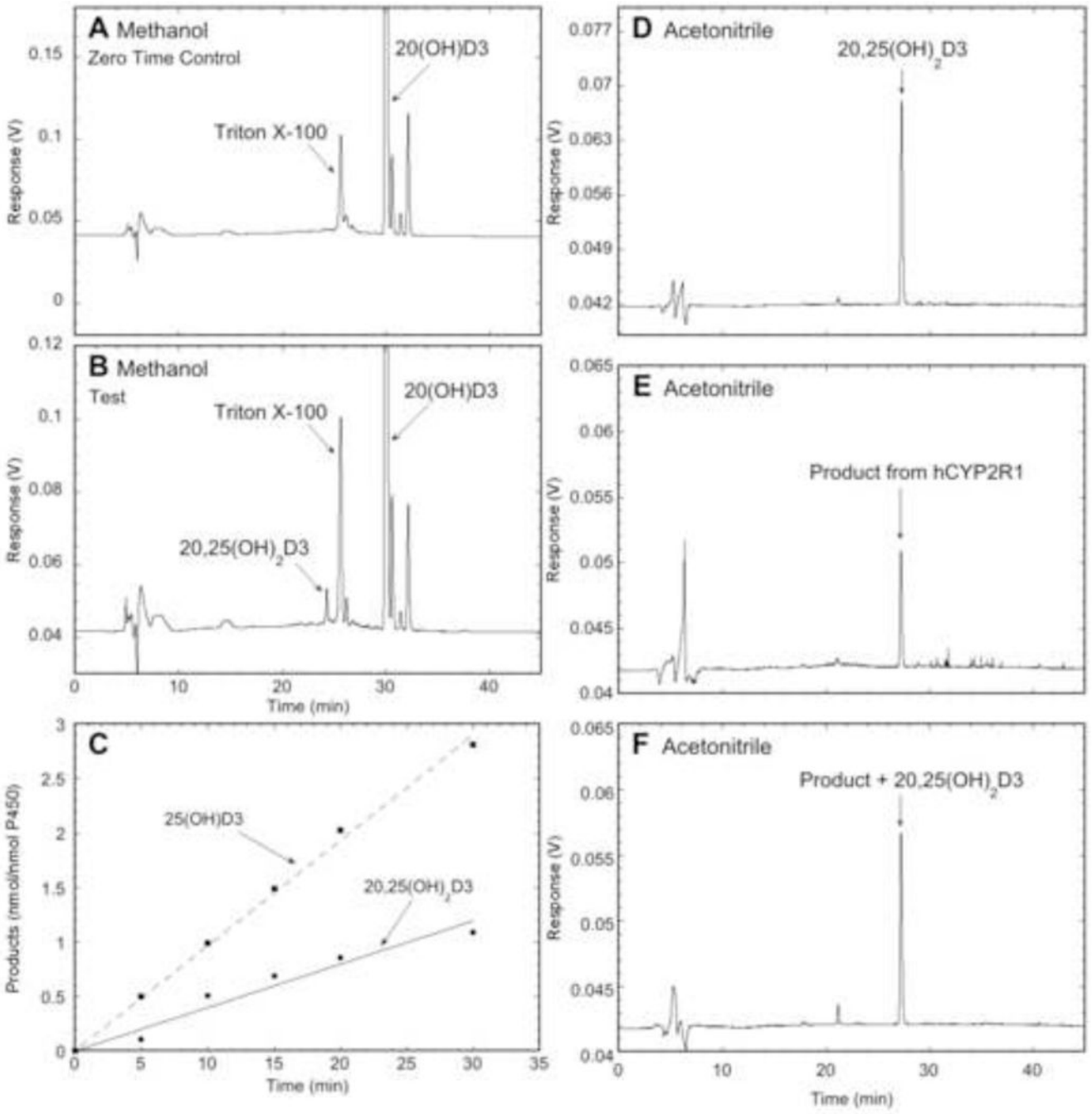

Fig. 3.

HPLC analysis and time course for metabolism of 20(OH)D3 by CYP2R1. 20(OH)D3 or vitamin D3 (0.1 mol/mol PL) was incubated with 0.25 μM CYP2R1, and the reactions started with 1.0 μM POR. Products were extracted and analyzed by reverse-phase HPLC. (A, B) Zero time control and test, respectively, for the metabolism of 20(OH)D3 by CYP2R1 after 60 min. The extract was chromatographed using a 64 – 100% methanol in water gradient for 15 min, followed by 100% methanol for 30 min, at 0.5 mL/min. The Triton X-100 peak originates from purified POR. (C) Time course for the metabolism of 20(OH)D3

and vitamin D3 by CYP2R1. Products were analyzed as for A and B except the 100% methanol step was extended to 40 min. (D, E, F) Further identification of major product from CYP2R1 action on 20(OH)D3 was carried out in a different solvent system comprising 45 – 100% acetonitrile in water for 30 min, followed by 100% acetonitrile for 35 min, at 0.5 mL/min. (D) 20,25$(OH)_2$D3 standard. (E) Major product collected from (B) corresponding to RT of authentic 20,25$(OH)_2$D3. (F) Major product collected from (B) spiked with 20,25$(OH)_2$D3 standard.

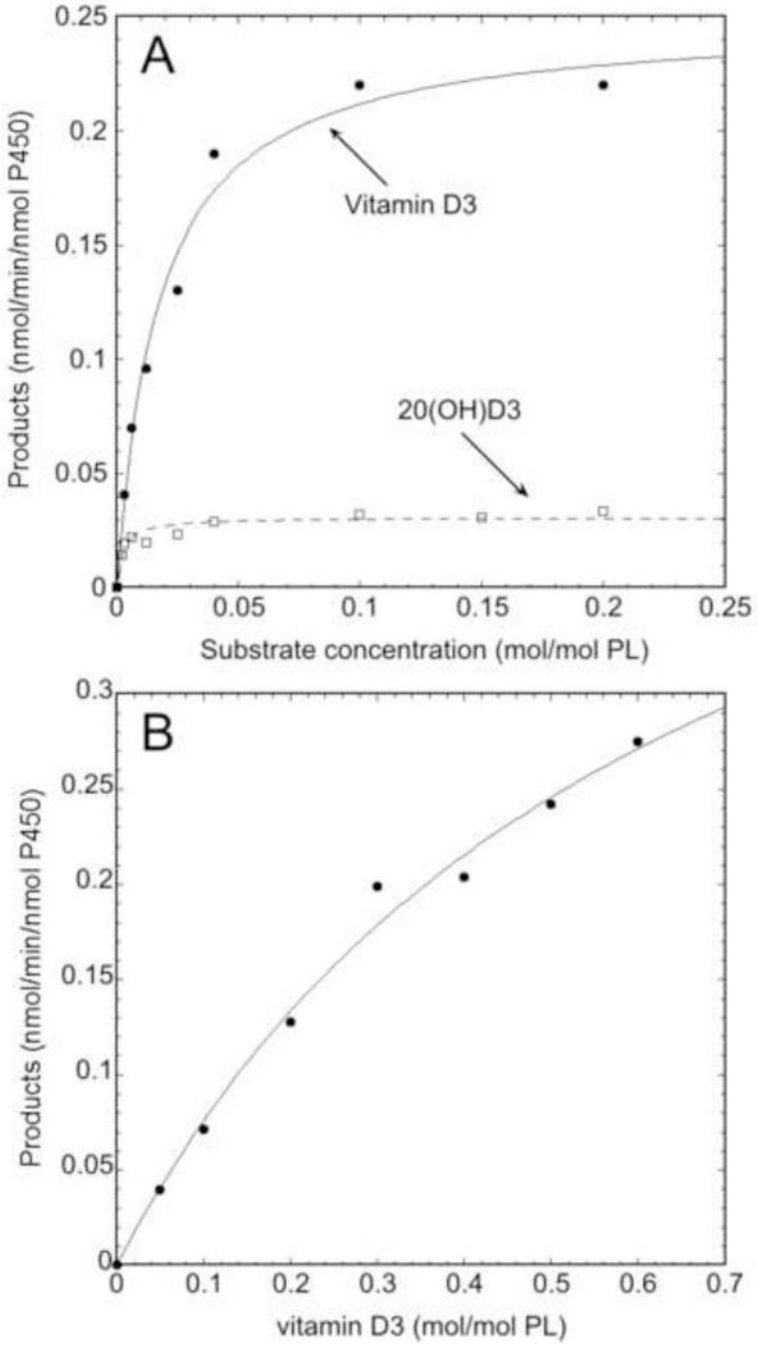

Fig. 4.

Kinetic analysis of the metabolism of vitamin D3 and 20(OH)D3 by CYP2R1 and vitamin D3 by CYP27A1. Vitamin D3 and 20(OH)D3 were incorporated into phospholipid vesicles and incubated with 0.25 μM CYP2R1 for 30 min or 0.2 μM CYP27A1 for 10 min. The products were extracted and analyzed as for Fig. 2 A,B. The Michaelis-Menten equation was fitted to experimental data using Kaleidagraph (Synergy software, version 4.5.2). (A) Comparison of kinetics for the metabolism of vitamin D3 and 20(OH)D3 by CYP2R1. (B) Kinetics for the metabolism of vitamin D3 by CYP27A1.

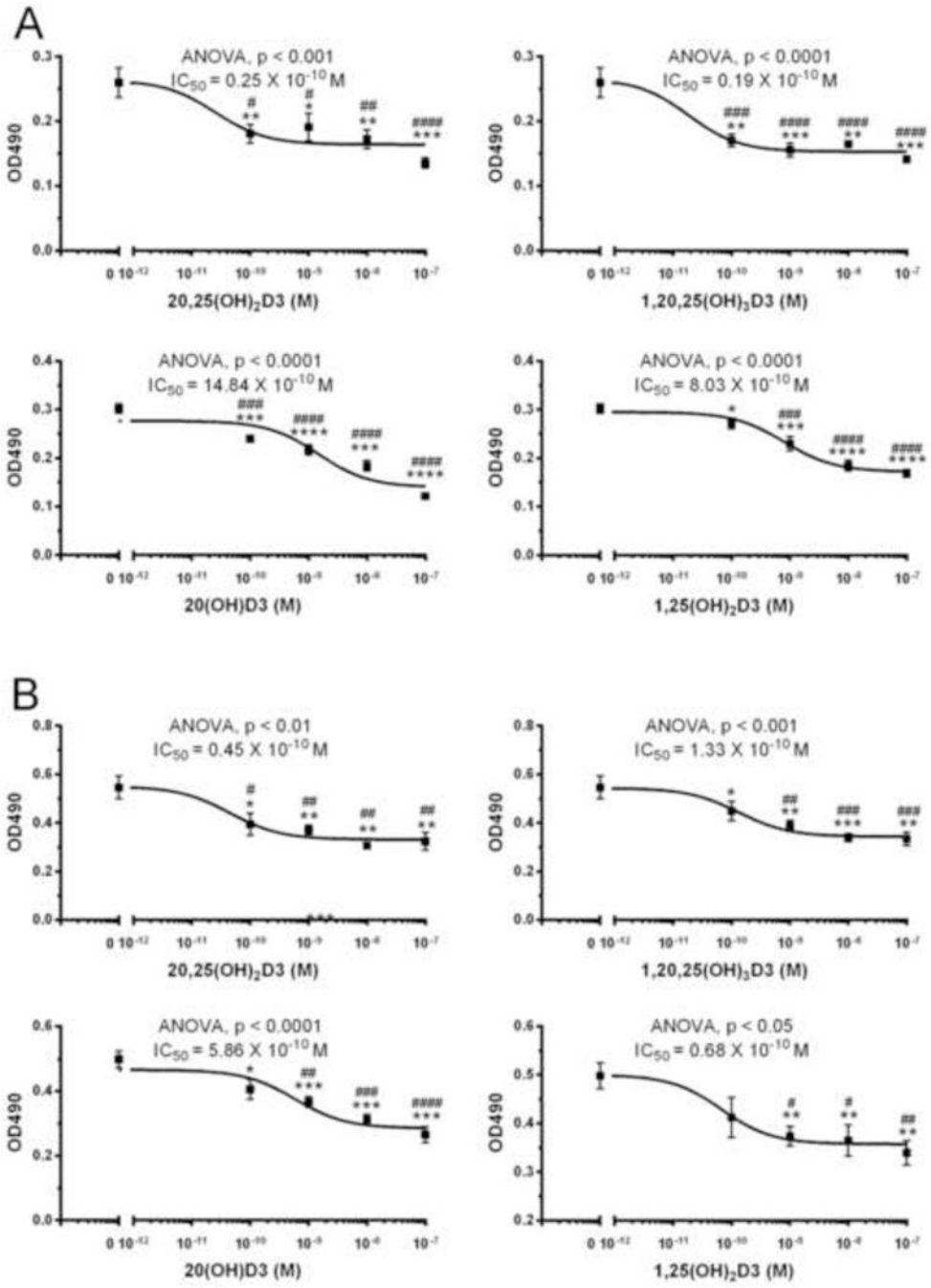

Fig. 5.

$20,25(OH)_2D3$ and related secosteroids inhibit the proliferation of melanocytes and dermal fibroblasts. The inhibition of proliferation of human melanocytes (A) and dermal fibroblasts (B) by $20,25(OH)_2D3$, $1,20,25(OH)_3D3$, 20(OH)D3 and $1,25(OH)_2D3$ was measured at 72 h of treatment using MTS reagent. Data are expressed as mean ± SE ($n \geq 4$). The statistical significance of differences were evaluated by Student's t test where *P < 0.05; **P < 0.01; ***P < 0.001; ****P < 0.001 and one-way ANOVA test where # $P < 0.05$; ## $P < 0.01$; ### $P < 0.001$; #### $P < 0.0001$. General ANOVA tests are shown on the panels.

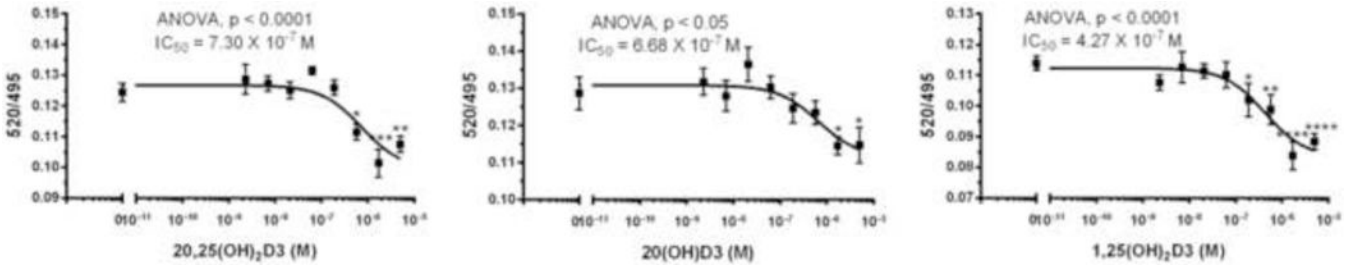

Fig. 6.

The interaction of 20,25$(OH)_2$D3 and related secosteroids with the RORα receptor. The RORα coactivator-binding assay was performed using LanthaScreen® TR-FRET ROR alpha Coactivator Assay Kit. The fluorescein emission at 520 nm and the Terbium emission at 495 nm were read using Synergy neo2 (BioTek Instruments, Inc. Winooski, VT), and the ratio was calculated. Data are shown as means ± SE (n > 3) where *p<0.05, **p<0.01, ***p<0.001 and ****p<0.0001 by the student t-test, and general ANOVA tests are shown on the panels.